The detection of microbes in Martian mudstone analogues using laser ablation ionization mass spectrometry at high spatial resolution

Andreas Riedo[1,2], Coen de Koning[1], Adam H. Stevens[3], Alison McDonald[4], Alena Cedeño López[5], Marek Tulej[2], Peter Wurz[2], Charles S. Cockell[3], and Pascale Ehrenfreund[1]

[1]Sackler Laboratory for Astrophysics, Leiden Observatory, Leiden University, Leiden, The Netherlands

[2]Space Research and Planetary Sciences, Physics Institute, University of Bern, Bern, Switzerland

[3]School of Physics and Astronomy, UK Centre for Astrobiology, University of Edinburgh, Edinburgh, United Kingdom

[4]School of Engineering, Bioimaging Facility, University of Edinburgh, Edinburgh, United Kingdom

[5]Department of Chemistry and Biochemistry, University of Bern, Bern, Switzerland

Corresponding Author: Andreas Riedo, Space Research and Planetary Sciences, Physics Institute, Sidlerstrasse 5, University of Bern, Switzerland

Phone: +41 31 631 30 71

E-Mail: andreas.riedo@space.unibe.ch

Running Title: LIMS detects microbes in Martian analogues

Abstract

The detection and identification of biosignatures on planetary bodies such as Mars is extremely challenging. Current knowledge from space exploration missions suggests that a suite of complementary instruments is required for a successful identification of past or present life. For future exploration missions, new and innovative instrumentation capable for high spatial resolution chemical (elemental and isotope) analysis of solids with improved measurement capabilities is of considerable interest because a multitude of potential signatures of extinct or extant life have dimensions on the micrometre scale. The aim of this study is to extend the current measurement capabilities of a miniature laser ablation ionisation mass spectrometer designed for space exploration missions to detect signatures of microbial life. In total, fourteen Martian mudstone analogue samples were investigated regarding their elemental composition. Half of the samples were artificially inoculated with a low number density of microbes and half were used as abiotic controls. The samples were treated in a number of ways. Some were cultured anaerobically and some aerobically; some abiotic samples were incubated with water and some remained dry. Some of the samples were exposed to a large dose of γ-radiation and some were left un-irradiated. While no significant elemental differences were observed between the applied sample treatments, the instrument showed the capability to detect biogenic element signatures of the inoculated microbes by monitoring biologically relevant elements, such as hydrogen, carbon, sulphur, iron, etc. When an enrichment in carbon was measured in the samples but no simultaneous increase in other biologically relevant elements was detected, it suggests carbon-grain inclusions; when the enrichment was in carbon and in bio-relevant elements, it suggests the presences of microbes. This study presents first results on the detection of biogenic element patterns of microbial life using a miniature LIMS system designed for space exploration missions.

Keywords: microbes, LIMS, space exploration, Mars, laser ablation ionisation mass spectrometry, high resolution chemical imaging

Introduction

The detection and identification of biosignatures on Mars are important challenges in Astrobiology and Space Science, see e.g., (Grotzinger *et al.* 2012; Vago *et al.* 2017; Westall *et al.* 2015). A positive detection would have a tremendous impact on the perception of our society, as the question "Is there life beyond Earth" could be answered, a "research topic" that started with the Viking missions on Mars in the 1970's, see e.g. (Klein 1978; Klein 1979; Soffen and Snyder 1976). Past and current missions have demonstrated that the *in situ* detection and identification of traces of life on Mars is extremely challenging. A positive detection of life will depend on many different factors, ranging from the selection of the most promising field site, which may host or preserve biomarkers, to the application of appropriate instrumentation, measurement capabilities and sensitivity.

Recently, the habitability and the potential for biosignature preservation in terrestrial analogues of five key Mars environments (hydrothermal spring systems, subaqueous environments, subaerial environments, subsurface environments, and iron-rich systems) were reviewed in detail (Hays *et al.* 2017). The review demonstrates the complexity of each environment and that a better understanding of currently available space instrumentation is required to determine what can be measured *in situ* on Mars. Complementary to the achievements of bulk chemical analysis methods conducted in the field sites, sensitive spectroscopic, spectrometric, and imaging instrumentation with micrometre-level spatial resolution are of high interest for future exploration missions. At best, the instrumentation should have the ability to e.g., differentiate biotic and abiotic signatures (Cady *et al.* 2003; Hays *et al.* 2017).

Various potential biosignatures and their response to time and change in environment have been discussed in literature, ranging from organic biomolecules (e.g. amino acids, lipids, etc.) to

microscopic structures (e.g. microfossils, cherts, etc.), see e.g. (Aerts *et al.* 2014; Boston *et al.* 2001; Cady *et al.* 2003; Marshall *et al.* 2017; Mustard *et al.* 2013; Vago *et al.* 2017). The Mars2020 Science Definition Team has identified six major groups of signatures of life; organic molecules, minerals, macro-structures and -textures, micro-structures and -textures, chemistry, and isotope fractionation (Mustard *et al.* 2013). Detecting and analysing the micro-scale structures, textures and chemistry of biological features such as biofilms, microfossils or even single organisms requires sensitive measurement techniques that provide spatial resolution at micrometre scale. Instrumentation designed for bulk chemical analysis might not detect micrometer-scale signatures because the specific chemical information of these features is not significant within the surrounding host material.

In this contribution, we present the current measurement capabilities of a miniature laser-ablation ionisation mass spectrometer (LIMS) for the detection of microbial life inoculated in an analogue of Martian mudstone. The system used is designed for *in situ* characterisation of the elemental and isotope composition of solid samples on planetary surfaces with a high spatial resolution (lateral and vertical resolution at the micro- and nanometre level, respectively), and has proven capabilities identifying e.g., putative micrometre-sized fossil structures embedded in a host mineral matrix (Tulej *et al.* 2015; Wiesendanger *et al.* 2018) and mineral phases within geological materials (Neubeck *et al.* 2015). The measurements conducted for this study demonstrate that identifying single cells is feasible using this instrument by monitoring major biological relevant elements.

Experimental

Sample Material and Preparation

The analogue material used in our sample preparation and the microbial inoculation is described in full detail in previous publications (Stevens *et al.* 2019; Stevens *et al.* 2018). Therefore, only a brief discussion is given below.

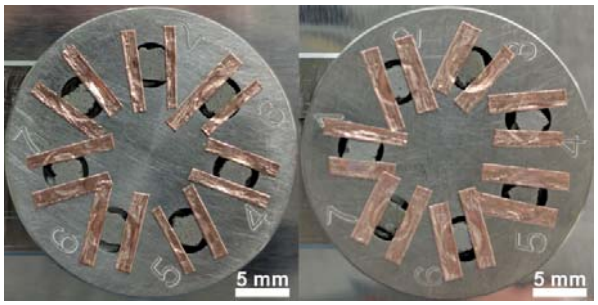

FIG. 1 Two LIMS sample holders are shown with the mudstone analogues installed. The materials were cut using a surgery blade in fragments of mm dimensions and fixed on the sample holders using ultra-high-vacuum compatible tape. A total of fourteen different samples were measured where half of the analogue materials contained microbes at low concentrations (on the order of ~10^6 cells/cm^3).

The Martian analogue mineral matrix, which is the same for all the samples investigated in this study, is an artificially produced Martian mudstone analogue (Y-Mars) that is a mixture of powdered commercially available minerals (Albite, Saponite, Augite, Magnetite, Enstatite, Dunite, Anhydrite, Sanidine, Pyrrhotite, and Selenite). These minerals were chosen to match *in situ* measurements of Martian drill samples (Vaniman *et al.* 2014).

In total 14 samples were investigated using LIMS. Half of the mudstone analogues were artificially inoculated with either an environmental microbial sample from a lake or a single species culture of *Bacillus subtilis* (on the order of ~10^6 cells/cm^3). Negative controls with no microbial inoculation were prepared with dry analogue material or with water under the same aerobic or anaerobic atmospheres. Following inoculation and culture under 96% N_2 / 4% CO_2 for nine months, samples were dried and pressed into pellets. The sample pellets were then exposed to different radiation conditions, with some samples receiving a dose of γ-radiation approximating doses in the near-surface of Mars. See (Stevens *et al.* 2019) for full details.

Various analytical techniques were used for the characterisation of the sample material, including DNA sequencing, bulk mass spectrometry, high-resolution Raman spectroscopy, and Fourier

transform infrared spectroscopy. The scientific findings using these techniques are discussed in detail in (Stevens *et al.* 2019), which concludes that only techniques offering sufficiently high spatial resolution allow for the detection of biological signatures from such samples.

For the LIMS analysis of the samples, the pellets were cut in mm-sized pieces and fixed in cavities on two sample holders using ultra-high-vacuum compatible copper tape. Sample handling and preparation was conducted in a clean room to avoid environmental contamination. Figure 1 shows the two sample holders with the accommodated samples. Table 1 gives an overview of the sample material investigated using the LIMS including sample treatment.

Tab 1: Investigated sample material and sample treatment.

Holder 1: biotic samples		**Holder 2: abiotic samples**	
H1S1	AN3I	H2S1	AEDI
H1S2	AN3I	H2S2	ANDI
H1S3	AN2I	H2S3	AEWI
H1S4	AN2U	H2S4	AEDU
H1S5	AN3U	H2S5	ANWU
H1S6	AN3U	H2S6	ANDU
H1S7	AN2U	H2S7	ANWI

AN: anaerobic; D: dry; U: un-irradiated; AE: aerobic; W: wet; I: irradiated

After LIMS analysis, Energy Dispersive X-ray (EDX) spectroscopy measurements (Hitachi, S300N instrument, working distance ~17.1 mm, acceleration voltage 25 kV, image size 512 x 384 px) were conducted on three samples (H1S2, H1S3, and H1S6, randomly selected) to investigate the porosity (voids) and chemical homogeneity of the mudstone analogues. In Figure 2 element maps of O, Al, and Si are shown of the sample H1S2. Some localised voids due to sample porosity are clearly

visible which may result, depending on their dimension, in a reduced LIMS signal during measurement. In those cases where a significant reduced signal was observed, the measurement was repeated at the same instrument setting at a new and fresh sample location. Further, while the element maps of Al and Si show a high chemical homogeneity of the samples, there are a few locations with slightly increased O. The latter may point to single mineral grains that may still be present in the Martian analogue material. Such mineral inclusions result in a temporally increased signal intensity of mineral specific elements using LIMS (Neubeck *et al.* 2015).

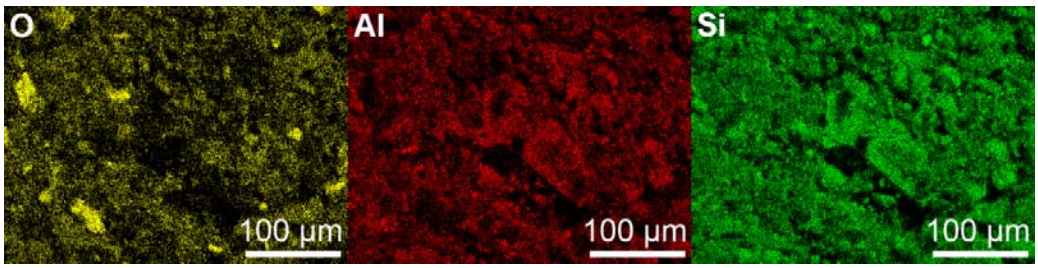

FIG. 2 EDX measurements of the sample material H1S2 after LIMS measurements. From left to right, the elemental maps of O, Al, and Si are shown.

LIMS measurement protocol

The measurement principles and figures of merit of the miniature LIMS system used in this study are discussed in detail in previous publications (Grimaudo *et al.* 2017; Grimaudo *et al.* 2015; Neubeck *et al.* 2015; Riedo *et al.* 2013a; Riedo *et al.* 2013b; Tulej *et al.* 2015; Wiesendanger *et al.* 2017; Wiesendanger *et al.* 2018). Therefore, only a brief description of the system is given in the following.

The LIMS system consists of a miniature (160 mm x Ø 60 mm) reflectron-type time-of-flight (R-TOF) mass spectrometer that is coupled to a femtosecond laser system (λ = 775 nm, 1 kHz laser pulse repetition rate) used for ablation and ionisation of sample material (Riedo *et al.* 2013a; Riedo *et al.* 2013b). The mass spectrometer is located inside a vacuum chamber with a typical base pressure

at the mid 10^{-8} mbar level. The laser system is located outside the vacuum chamber and a beam guiding system is used for beam delivery to the mass spectrometer. A lens system installed just above the mass spectrometer, inside the vacuum chamber, allows focusing the laser pulses through the mass spectrometer towards the sample surface to spot-sizes with a diameter in the range of about 10 – 20 µm (depending on sample material and applied laser pulse energy). The sample holders are placed on a 3D translation stage with a position accuracy of ~2 µm. A microscope camera system with resolving power of 1 µm allows accurate positioning of the samples below the mass spectrometer (Wiesendanger *et al.* 2018). Each laser pulse induces material ablation and ionisation, and only positively charged species can enter the mass spectrometer. After acceleration, confinement and focussing of the ions towards the field free drift path the ions are reflected at the ion mirror towards the detector system (Riedo *et al.* 2017) by passing a second time the field-free drift path. The ions arrive in time sequences at the detector system according to their mass-to-charge ratio (time-of-flight measurement principle, separation occurs in the field free drift paths) (Riedo *et al.* 2013a). A high-speed analogue-to-digital-converter card is used for signal acquisition (2 channels, each with a sampling speed of up to 2 GS/s, 8 bit vertical resolution). An in-house written software suite (Matlab) is used for the conversion between TOF to mass spectra and subsequent data analysis. A detailed description of the software can be found in a recent publication (Meyer *et al.* 2017).

As the primary goal of this study was the detection of elemental signatures of microbial cells within the mudstone analogue, the same measurement methodology based on spot-wise chemical depth profiling was used as developed earlier for the same LIMS instrument (Grimaudo *et al.* 2015). This measurement protocol has previously been applied to successfully identify fossil structures of micrometre dimensions in a host mineral matrix by monitoring biologically relevant elements (Tulej *et al.* 2015; Wiesendanger *et al.* 2018), mineral phases in geological sample by monitoring mineral specific elements (Neubeck *et al.* 2015), and layering structures of nanometre dimensions containing

residues of additives used in the electroplating processes (Moreno-García *et al.* 2016; Riedo *et al.* 2015). In this measurement protocol, a number of TOF spectra (here 500) are accumulated first onboard by the data acquisition card and subsequently saved as one file on the host computer. In this study, at each instrument setting 60'000 laser shots were applied on a new sample location, resulting in 120 accumulated TOF files. Each file represents a layer of ablated sample material and knowing that tens of micrometres are ablated with this number of total laser shots, each layer has a thickness of hundreds of nanometres to a few micrometres, depending on the used laser power (Tulej *et al.* 2015). Using this measurement principle, a laser irradiance campaign was conducted on each sample, with laser powers of 29, 34, 41, 49, 59, 69, 77 mW (corresponding to laser pulse energies at sample surface of ~0.7 – 1.7 µJ), that allows the identification of optimal conditions for signal-to-noise and mass resolution. Measurements conducted at laser powers in the range of 34 mW – 69 mW (pulse energy of ~0.8 – 1.6 µJ) showed best measurement results and were used for subsequent data analysis.

Results and Discussion

Bulk chemical analysis

The measurement procedure discussed above allows us not only to have a spatially resolved chemically information of the investigated sample, but also to have a bulk view of the chemical composition by accumulating a large number of such files from the same surface position (Neuland *et al.* 2018; Neuland *et al.* 2014). Small variations in signal intensities, due to e.g. sample morphology and local mineralogy, are averaged out by this procedure, which increases the reliability of chemical information. This accumulation of a large number of such files was conducted to investigate if any differences between the sample treatments can be observed (wet to dry, anaerobic to aerobic, irradiated to unirradiated).

In Figure 3 a typical overview mass spectrum for the mass range of interest - carbon to iron – of sample H2S6 (abiotic, dry, unirradiated) is shown. Here, the mass spectrum is an accumulation of 71 files, which corresponds to a total accumulation of 35'500 single mass spectra (71 x 500 mass spectra). Spectra that showed a poor mass resolution, mainly resulting from local porosity of the material or observed at the early stages of formation of the laser ablation crater, were removed (Wiesendanger *et al.* 2019). In this representation all major to minor elements, such as O, Si, to Fe, can be observed. By zooming in the data, even the trace elements at the ppm level, such as phosphorus with around 60 ppm abundance (atomic fraction, at fract.), are clearly visible (see inset).

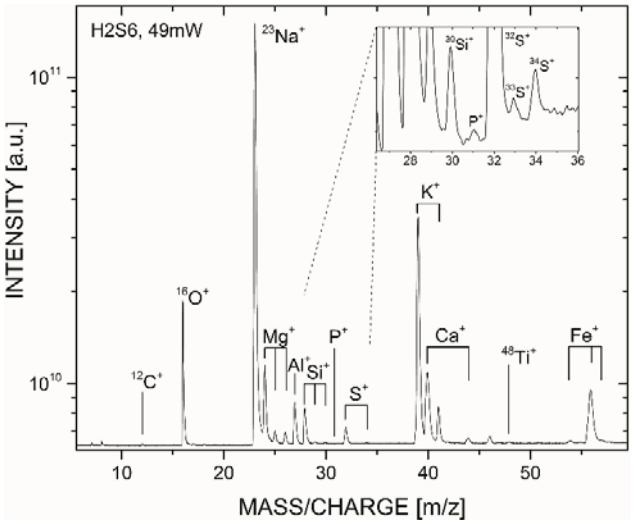

FIG. 3 Typical overview mass spectrum of the Martian analogue matrix showing the mass range of interest between carbon and iron. Here, the shown mass spectrum is an accumulation of 71 files, each consisting of 500 spectra, which results in a total compilation of 35'500 LIMS spectra. In the inset, showing the mass/charge range of ~27 – 36, phosphorus with an abundance of ~60 ppm abundance (at. fract.) is clearly visible.

No significant differences in the elemental composition of the samples using different treatments were observed. Comparing wet and dry sample treatments, no increased H or O abundance was observed, as expected. Since the measurements were conducted under vacuum conditions (at the 10^{-8} mbar level), all remaining residual water in the mudstone analogue should have evaporated before

the measurements. The same holds for the case of anaerobic and aerobic sample handling: no significant difference in the abundance of O was detected. Moreover, gaseous oxygen is not expected to change the atomic element composition of the mudstone analogue, which is in line with our observation.

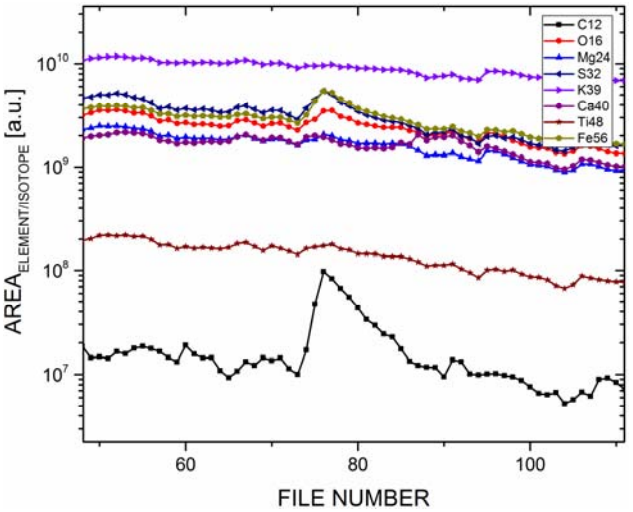

FIG. 4 Peak area variations of a group of elements as function of depth, i.e., the recorded file number. Slight element variations are expected, given the nature of the sample, but around file number 76 carbon shows a tenfold increase in intensity whereas the other elements stay almost constant (note the logarithmic scaling). This element monitoring allows the identification of regions of interest, here a carbon-rich layer.

Identification of carbon rich layers

In analytical measurement techniques using laser ablation ion sources, e.g., Laser Induced Breakdown Spectroscopy (LIBS), Laser Ablation Ionisation Mass Spectrometry (LIMS), or Laser Ablation Inductively Coupled Mass Spectrometry (LA-ICP-MS), shot-to-shot signal variations are expected, see e.g. (Cui *et al.* 2012; De Bonis *et al.* 2014; Gutierrez-Gonzalez *et al.* 2015). Such variations may arise from various factors, including instability of the used laser system, sample morphology and porosity (voids), local variations in chemical composition, among others. Fortunately, in the instrument setup used in this study, the factor "laser stability" is negligible as the

system has an excellent pulse-to-pulse energy stability in the per mill range. Therefore, changes in the observed signal intensities can be attributed to changes in the chemistry of the investigated sample.

Contrary to the bulk chemical analysis of the mudstone analogue shown in Fig. 3, the advantage of the chemical depth profiling measurement methodology is demonstrated in Fig. 4. Here, intensity variations of a subset of user-defined elements within a recorded file range of ~50 – 110 are shown. Using this measurement procedure, regions of scientific interest can be identified and the subset of measured data can be used to further investigate the local chemical composition; contributions from the mudstone analogue can be therefore reduced.

As the main goal of this study is the localisation of microbial life in the sample, we have chosen the element carbon for data screening as this element is abundant in bacterial life and is not supposed to be present in the mudstone analogue (see used minerals to simulate the Martian mudstone). In Figure 4 (note the logarithmic scale), we observe an increase in signal intensity of carbon of about ten times at file number 76, compared the measurements above and below the localised carbon increase. Other major elements remain at about the same intensity. Note, that the observed peak-like shape is induced due to a moving average window, which was applied for easier identification of such localised signal increase. The significant increase of carbon signal points to a location in the sample highly enriched in carbon. Since the laser pulses are focussed to spot sizes of about 20 µm in diameter any object within that lateral dimensions can introduce such an increase in signal intensity. The ablated material of that irradiated zone consists almost solely of that chemical composition which may be different with respect of the surrounding analogue material. However, at this stage, this carbon enrichment cannot be attributed to a biological origin. For a conclusive interpretation of this carbon rich layer the mass spectrum of this layer needs to be investigated in more detail.

The mass spectrum for a carbon-rich layer described in Fig 4. is shown in Fig. 5. In red (pointing down) the mass spectrum of the layer enriched in carbon is shown, whereas in black and blue (pointing up) the mass spectra of the surrounding mudstone analogue, above and below the observed carbon rich layer (accumulation of 10 layers) are displayed for comparison. As can be clearly observed, carbon is the only element significantly increased relative to the surrounding analogue material and other element intensities remain about the same. Note that the spectra of the analogue measured above and below the carbon rich layer are almost identical which underlines the stability of our LIMS measurements. As no significant changes in other element intensities are observed, the mass spectrum of the carbon-rich layer points to the detection of a carbon grain inclusion rather than to a local inhomogeneity of the analogue material.

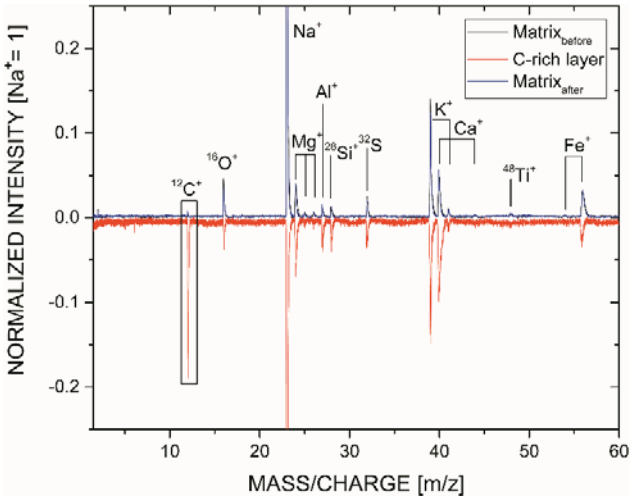

FIG. 5 Mass spectra of a carbon-rich layer (in red) and of surrounding analogue material (black: accumulation of 10 files above carbon-rich layer, blue: accumulation of 10 files below carbon-rich layer) are shown. Here, only a significant increase of carbon can be observed whereas the intensities of the other elements remain about the same level.

Identification of biologically relevant inclusions

In Figure 6, a mass spectrum from another carbon rich layer is shown. Similar to Fig. 5, the carbon-rich layer is displayed in red whereas the surrounding analogue in black and blue. Again, both analogue spectra measured above and below the carbon-rich layer agree with each other very well, as no significant differences in element intensities can be observed. In the carbon layer, however, we observe a significant increase of biologically relevant elements, such as H, S, and Fe. Careful inspection of the mass spectrum shows an increase in the less abundant elements such as N and P as well (see insets at the bottom layer). Note that for these parts of the spectrum shown for N and P a moving average filter (30 and 40 data points for N and P, respectively) was used for noise filtering as the spectrum represents only one layer (reduced statistics), in contrast to the spectra of the mudstone analogue which consist of a compilation of 10 layers.

In total, eight layers significantly enriched in carbon in comparison to the analogue material were identified (like in Figs. 5 and 6) during the conducted measurements. We could not identify a significant trend between sample treatments, such as wet or dry, anaerobic or aerobic, or the applied laser pulse energy. Further, the carbon-rich layers were found distributed over a range of measurement layers (crater depths), rather than only at a certain depth or only at the top surface. In the latter case, the carbon could be attributed to sample surface contamination during sample preparation or handling. Of these eight cases, five were found in biotic samples whereas the remaining three were detected in abiotic ones. Figure 6 shows a typical case for the biotic sample material whereas Fig. 5 shows a typical case of an abiotic sample.

For the samples containing microbial communities, four out of five showed a significant and simultaneous increase of major and minor biologically relevant elements H, O, S, and Fe in the carbon rich layers (Wackett *et al.* 2004). In the final case, the abundance of H, C, S, and Fe are observed to increase simultaneously, while O decreased slightly. This behaviour might be explained

by oxygen-rich surrounding analogue material (XRD measurements showed atomic fractions at the level of ~60%), which could give the impression of a decreasing oxygen content. In all abiotic samples, only the significant increase of carbon was observed, while all other elements stayed constant in comparison to the surrounding mudstone analogue. This means that no false positive detection of microbial life was detected in an abiotic sample.

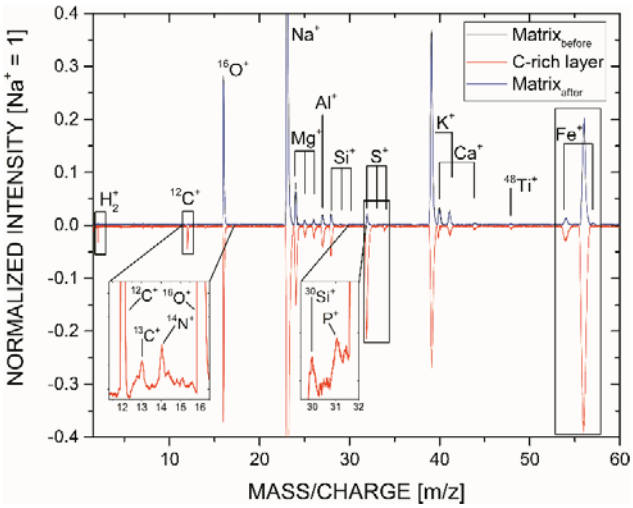

FIG. 6 Mass spectra of a carbon-rich layer (in red) where a simultaneous increase of biogenic elements such as H, N, P, S, and Fe is observed. Upwards (in blue and black) the mass spectra of ten accumulated layers above and below the carbon-rich layer are displayed additionally for comparison. Note the high measurement reproducibility of both analogue spectra; no significant deviations in other elements can be observed.

Knowing that the Martian analogue materials for all investigated samples were identical and that the only difference between biotic and abiotic samples was the presence of microbes, the consistency of finding layers with significant increased abundances of biologically relevant elements exclusively in analogues containing microbes strongly implies that biological material was detected reliably. Furthermore, the number of positive detections, assuming that a detection represents a single microbe, is close to the occurrence of microbes within the sample material (on the order of around 10^6 cells/cm^3) and the number of conducted measurements. In total 4 measurements were conducted

on each biotic material (at 4 different pulse energies); on each biotic sample a total volume of about 4 x 10^{-7} cm^3 was investigated (for crater diameter of ~20 µm, depth of about 50 µm, pitch between each measurement was 100 µm). Therefore, a total volume of ~2.8 x 10^{-6} cm^3 over all biotic materials was investigated. In that estimated ablated volume around 2 – 3 cells should be detected, which compares well with our 5 detections. This low number of positive detections is further in line with a complementary study comparing various analysis methods (Stevens *et al.* 2019), which reported that bulk mass spectrometric analysis showed no indications of microbes, similar to other methods investigating the bulk properties. Only spatially resolved sensitive measurement techniques like high-resolution Raman spectroscopy and here LIMS, identified a biogenic signature. Note, that if we would accumulate all our mass spectra in one final mass spectrum, i.e., emulating a bulk analysis, we also would not see biogenic signatures. On the other hand, we might assume that the observed elemental pattern belongs to a carbon-containing mineral. However, we screened the mineral database *mindat.org* in search for minerals containing the elements with a significant increase (here H, C, S, Fe; O is not included as it showed in one sample a slightly decreasing trend, see comments above) and found only minerals containing additional other specific elements, such as Zn, which do not match our observations.

Figure 7 shows the intensity variations of a subset of elements of the special case of the detection of two subsequent biotic layers. Here, layers 2 and 4 correspond to the biotic layer and layers 1 (accumulation of 10 layers above carbon-rich layer), 3 (accumulation of 9 layers above next carbon-rich layer), and 5 (accumulation of 10 layers below carbon-rich layer) to the surrounding analogue material. In the top row, the intensities of the most significant elements H, C, and S are shown. The variations between both biotic and abiotic layers can be clearly observed in these elements, and the element intensities detected for both layer types are highly reproducible in view of the nature of these samples. In the second row, the intensities of Mg, O, and Fe are displayed. The elements Mg and Fe follow the same trend as the elements H, C, and S since they participate in the chemistry of

living organisms. However, and as stated earlier in the text, O shows a consistent but opposite trend by means of a decreased element abundance in the biotic layer. This observation may be attributed to the fact that O is highly abundant in the analogue material at about ~60% (atomic fraction) whereas in biotic material the O abundance is about 20%, thus the overall measured abundance appears to be lower. A similar trend is observed for K (i.e., a decrease of K in the carbon-rich layer, see Fig. 6), which can be attributed to the lower K abundance in microbes compared to the mineral analogue.

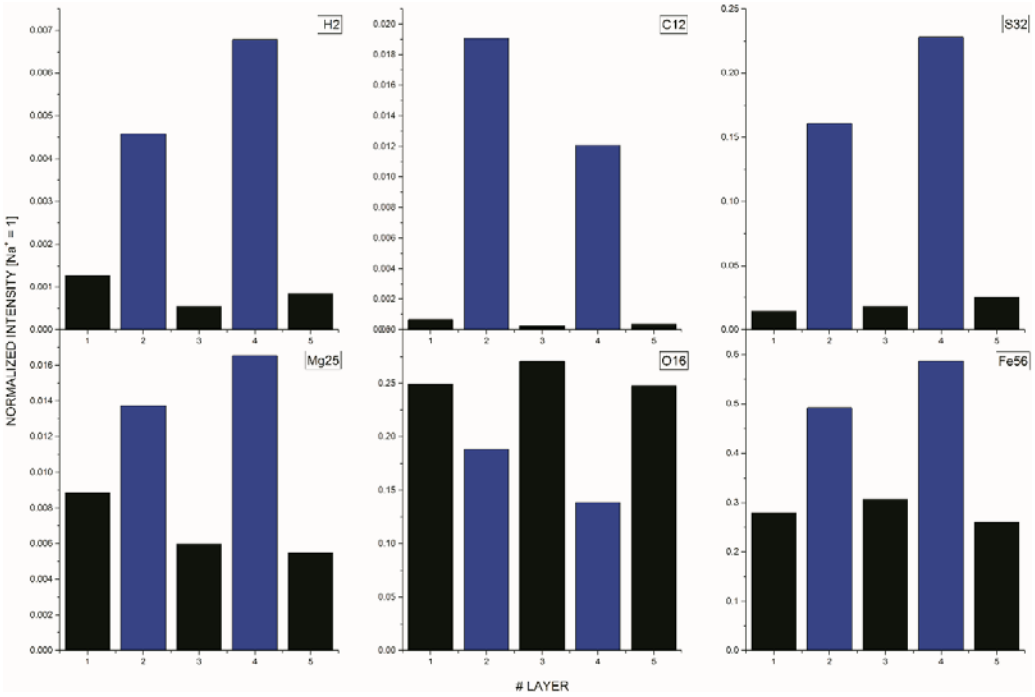

FIG. 7 Intensities of biologically relevant elements, H, C, S, Mg, O and Fe between abiotic (black) and biotic (blue) layers are shown. All but O follow the same trend of increased abundances at biotic layers.

Conclusions

Past and current in situ space exploration missions devoted to the detection of biogenic signatures of extinct or extant life on Mars have shown that identifying biosignatures is extremely challenging.

Multi-instrument efforts are required to provide conclusive results if a potentially detected signature is of biotic nature or is induced by geochemical processes. Various laboratory studies have further shown the necessity of sensitive measurement techniques providing information on the chemical composition of solids with high spatial resolution at the micrometre level. Biosignatures, or remnants of life, can be expected at these spatial dimensions, including e.g. fossilised structures, cherts, microbial life, etc.

In this contribution, Martian mudstone analogues that were exposed to wet or dry, anaerobic or aerobic, irradiated or unirradiated, and abiotic or biotic conditions were chemically (elements) analysed with a spatial resolution at the micrometre level using a miniature LIMS system that is designed for in situ space exploration. Whereas no significant differences in the element composition between different sample treatments were identified, the chemical depth profiling measurement protocol, allowed the identification of biotic and abiotic carbon-rich layers within the investigated sample material. In abiotic layers, a significant increase of carbon was detected whereas the other elements remained constant in concentration (with the surrounding analogue material). In biotic layers the signal intensities of various biologically relevant elements, including e.g. H, C, N, S, increased simultaneously. With the knowledge that the only difference between biotic and abiotic samples is the presence of microbes at low number density strongly implies that microbial life was detected. Furthermore, the number of biotic detections is in line with the estimated density of microbes in the analysed material. Therefore, with the knowledge of the chemical composition of the Martian analogue (considered as background, averaging over the entire measurement campaign) and a potential observation of a simultaneous increase of elements associated with biology may allow a reliable in situ identification of microbial life.

These detections were only possible because of the high detection sensitivity of the miniature LIMS system coupled with the measurement capability to chemically investigate a solid with a spatial

resolution at the micrometre level. For future studies, it is planned to investigate potential isotope signatures of biologically relevant elements to complement the elemental analysis discussed in this contribution. Nevertheless, the presently accomplished capability is highly promising for the detection of microbial life at micrometre dimensions on planetary surfaces. A measurement suite that combines high-resolution imaging and chemical composition analysis at micrometre level, such as the presented LIMS system, would be advantageous for future space exploration missions devoted to the detection of signatures of life at micrometre dimensions.

Acknowledgments

AR acknowledges the support from the European Union's Horizon 2020 research and innovation programme under the Marie Skłodowska-Curie grant agreement No. 750353. PW acknowledges the support by the Swiss National Science foundation (SNSF). AHS and CSC were supported by Science and Technology Facilities Council grant No. ST/R000875/1

Author Disclosure Statement

No competing financial interests exist.

References

Aerts J., Röling W., Elsaesser A., and Ehrenfreund P. (2014) Biota and Biomolecules in Extreme Environments on Earth: Implications for Life Detection on Mars. *Life*, 4: 535.

Boston P. J., Spilde M. N., Northup D. E., Melim L. A., Soroka D. S., Kleina L. G., Lavoie K. H., Hose L. D., Mallory L. M., Dahm C. N. and others. (2001) Cave Biosignature Suites: Microbes, Minerals, and Mars. *Astrobiology*, 1: 25-55.

Cady S. L., Farmer J. D., Grotzinger J. P., Schopf J. W., and Steele A. (2003) Morphological Biosignatures and the Search for Life on Mars. *Astrobiology*, 3: 351-368.

Cui Y., Moore J. F., Milasinovic S., Liu Y., Gordon R. J., and Hanley L. (2012) Depth profiling and imaging capabilities of an ultrashort pulse laser ablation time of flight mass spectrometer. *Review of Scientific Instruments*, 83: 093702.

De Bonis A., De Filippo B., Galasso A., Santagata A., Smaldone A., and Teghil R. (2014) Comparison of the performances of nanosecond and femtosecond Laser Induced Breakdown Spectroscopy for depth profiling of an artificially corroded bronze. *Applied Surface Science*, 302: 275-279.

Grimaudo V., Moreno-García P., Riedo A., Meyer S., Tulej M., Neuland M. B., Mohos M., Gütz C., Waldvogel S. R., Wurz P. and others. (2017) Toward Three-Dimensional Chemical Imaging of Ternary Cu–Sn–Pb Alloys Using Femtosecond Laser Ablation/Ionization Mass Spectrometry. *Analytical Chemistry*, 89: 1632-1641.

Grimaudo V., Moreno-García P., Riedo A., Neuland M. B., Tulej M., Broekmann P., and Wurz P. (2015) High-Resolution Chemical Depth Profiling of Solid Material Using a Miniature Laser Ablation/Ionization Mass Spectrometer. *Analytical Chemistry*, 87: 2037-2041.

Grotzinger J. P., Crisp J., Vasavada A. R., Anderson R. C., Baker C. J., Barry R., Blake D. F., Conrad P., Edgett K. S., Ferdowski B. and others. (2012) Mars Science Laboratory Mission and Science Investigation. *Space Science Reviews*, 170: 5-56.

Gutierrez-Gonzalez A., Gonzalez-Gago C., Pisonero J., Tibbetts N., Menendez A., Velez M., and Bordel N. (2015) Capabilities and limitations of LA-ICP-MS for depth resolved analysis of CdTe photovoltaic devices. *Journal of Analytical Atomic Spectrometry*, 30: 191-197.

Hays L. E., Graham H. V., Marais D. J. D., Hausrath E. M., Horgan B., McCollom T. M., Parenteau M. N., Potter-McIntyre S. L., Williams A. J., and Lynch K. L. (2017) Biosignature Preservation and Detection in Mars Analog Environments. *Astrobiology*, 17: 363-400.

Klein H. P. (1978) The Viking biological experiments on Mars. *Icarus*, 34: 666-674.

Klein H. P. (1979) The Viking mission and the search for life on Mars. *Reviews of Geophysics*, 17: 1655-1662.

Marshall C. P., Marshall A. O., Aitken J. B., Lai B., Vogt S., Breuer P., PhilippeSteemans, and Lay P. A. (2017) Imaging of Vanadium in Microfossils: A New Potential Biosignature. *Astrobiology*, 17: 1069-1076.

Meyer S., Riedo A., Neuland M. B., Tulej M., and Wurz P. (2017) Fully automatic and precise data analysis developed for time-of-flight mass spectrometry. *Journal of Mass Spectrometry*, 52: 580-590.

Moreno-García P., Grimaudo V., Riedo A., Tulej M., Neuland M. B., Wurz P., and Broekmann P. (2016) Towards Structural Analysis of Polymeric Contaminants in Electrodeposited Cu films. *Electrochimica Acta*, 199: 394-402.

Mustard J. F., Adler M., Allwood A., Bass D. S., Beaty D. W., Bell III J. F., Brinckerhoff W. B., Carr M., Des Marais D. J., Drake B. and others. (2013) Report of the Mars 2020 Science Definition Team. 154.

Neubeck A., Tulej M., Ivarsson M., Broman C., Riedo A., McMahon S., Wurz P., and Bengtson S. (2015) Mineralogical determination in situ of a highly heterogeneous material using a miniaturized laser ablation mass spectrometer with high spatial resolution. *International Journal of Astrobiology*, 15: 133-146.

Neuland M., Mezger K., Riedo A., Tulej M., and Wurz P. (2018) The chemical composition and homogeneity of the Allende matrix. *Meteoritics and Planetary Sciences*, submitted.

Neuland M. B., Meyer S., Mezger K., Riedo A., Tulej M., and Wurz P. (2014) Probing the Allende meteorite with a miniature laser-ablation mass analyser for space application. *Planetary and Space Science*, 101: 196-209.

Riedo A., Bieler A., Neuland M., Tulej M., and Wurz P. (2013a) Performance evaluation of a miniature laser ablation time-of-flight mass spectrometer designed for in situ investigations in planetary space research. *Journal of Mass Spectrometry*, 48: 1-15.

Riedo A., Grimaudo V., Moreno-Garcia P., Neuland M. B., Tulej M., Wurz P., and Broekmann P. (2015) High depth-resolution laser ablation chemical analysis of additive-assisted Cu electroplating for microchip architectures. *Journal of Analytical Atomic Spectrometry*, 30: 2371-2374.

Riedo A., Neuland M., Meyer S., Tulej M., and Wurz P. (2013b) Coupling of LMS with a fs-laser ablation ion source: elemental and isotope composition measurements. *Journal of Analytical Atomic Spectrometry*, 28: 1256-1269.

Riedo A., Tulej M., Rohner U., and Wurz P. (2017) High-speed microstrip multi-anode multichannel plate detector system. *Review of Scientific Instruments*, 88: 045114.

Soffen G. A., and Snyder C. W. (1976) The First Viking Mission to Mars. *Science*, 193: 759.

Stevens A. H., McDonald A., Koning C. d., Riedo A., Wurz P., Ehrenfreund P., and Cockell C. S. (2019) Profound difficulties of biosignature detection in martian environments: are we equipped to find life on Mars? . *Scientific Reports*: submitted.

Stevens A. H., Steer E., McDonald A., Amador E. S., and Cockell C. S. (2018) Y-Mars: An Astrobiological Analogue of Martian Mudstone. *Earth and Space Science*, 5: 163-174.

Tulej M., Neubeck A., Ivarsson M., Riedo A., Neuland M. B., Meyer S., and Wurz P. (2015) Chemical Composition of Micrometer-Sized Filaments in an Aragonite Host by a Miniature Laser Ablation/Ionization Mass Spectrometer. *Astrobiology*, 15: 669-682.

Vago J. L., Westall F., Pasteur Instrument Teams L. S. S. W. G., Contributors O., Coates A. J., Jaumann R., Korablev O., Ciarletti V., Mitrofanov I., Josset J.-L. and others. (2017) Habitability on Early Mars and the Search for Biosignatures with the ExoMars Rover. *Astrobiology*, 17: 471-510.

Vaniman D. T., Bish D. L., Ming D. W., Bristow T. F., Morris R. V., Blake D. F., Chipera S. J., Morrison S. M., Treiman A. H., Rampe E. B. and others. (2014) Mineralogy of a Mudstone at Yellowknife Bay, Gale Crater, Mars. *Science*, 343.

Wackett L. P., Dodge A. G., and Ellis L. B. M. (2004) Microbial Genomics and the Periodic Table. *Applied and Environmental Microbiology*, 70: 647-655.

Westall F., Foucher F., Bost N., Bertrand M., Loizeau D., Vago J. L., Kminek G., Gaboyer F., Campbell K. A., Bréhéret J.-G. and others. (2015) Biosignatures on Mars: What, Where, and How? Implications for the Search for Martian Life. *Astrobiology*, 15: 998-1029.

Wiesendanger R., Tulej M., Grimaudo V., Cedeño-López A., Lukmanov R., Riedo A., and Wurz P. (2019) A method for improvement of mass resolution and isotope accuracy for laser ablation time-of-flight mass spectrometers. *Journal of Chemometrics*, 33: e3081.

Wiesendanger R., Tulej M., Riedo A., Frey S., Shea H., and Wurz P. (2017) Improved detection sensitivity for heavy trace elements using a miniature laser ablation ionisation mass spectrometer. *Journal of Analytical Atomic Spectrometry*, 32: 2182-2188.

Wiesendanger R., Wacey D., Tulej M., Neubeck A., Ivarsson M., Grimaudo V., Moreno P., Cedeño López A., Riedo A., and Wurz P. (2018) Chemical and optical identification of micrometre sized 1.9 billion-year-old fossils by combining a miniature LIMS system with an optical microscope.